

# Controlled Synthesis of Nonspherical Microparticles Using Microfluidics

Dhananjay Dendukuri, Kim Tsoi, T. Alan Hatton, and Patrick S. Doyle\*

Department of Chemical Engineering, Massachusetts Institute of Technology,  
77 Massachusetts Avenue, Cambridge, Massachusetts 02139

Received October 26, 2004. In Final Form: January 21, 2005

The controlled synthesis of nonspherical microparticles using microfluidics processing is described. Polymer droplets, formed by shearing a photopolymer using a continuous water phase at a T-junction, were constrained to adopt nonspherical shapes by confining them using appropriate microchannel geometries. Plugs were obtained by shearing the polymer phase at low shear rates, while disks were obtained by flattening droplets using a channel of low height. The nonspherical shapes formed were permanently preserved by photopolymerizing the constrained droplets in situ using ultraviolet light. Monodisperse plugs and disks of different lengths and diameters were obtained by varying the flow rates of the two phases.

## Introduction

The controlled synthesis of particles in the size range from 10 nm to 1000  $\mu\text{m}$ , comprising the colloidal length scale<sup>1</sup> ( $< 10 \mu\text{m}$ ) and larger length scales, is an important goal. Particles from across this length spectrum (which we shall refer to as microparticles) are used in diverse applications ranging from optical pigments to photonic materials and field-responsive rheological fluids. Monodisperse microparticles are particularly desirable as they exhibit a constant and predictable response to external fields and enable the particles to assemble into homogeneous crystal structures, thus aiding in the study of the bulk properties of assemblies of such materials.<sup>2,3</sup> To date, the study of microparticles has been dominated by spherical systems, mainly because the minimization of interfacial energy leads to the formation of spherical shapes during most syntheses, whether they are polymer latexes formed through emulsion polymerization<sup>3</sup> or droplets formed using shearing flows in microfluidic channels.<sup>4–6</sup> Few methods are available for the controlled synthesis of nonspherical microparticles, even though such particles are interesting for a variety of reasons. The properties conferred on assemblies of such materials by their lack of spherical symmetry could be exploited to synthesize materials with unique crystal structures<sup>2</sup> or to create materials that exhibit novel responses to external fields (e.g., an applied shear field<sup>7</sup> or electric field). Such microparticles could find diverse applications as the components of new field-responsive fluids and photonic materials,<sup>2</sup> as probes to explore the rheological properties of complex materials,<sup>8</sup> or as model systems to mimic anisotropic biological cells and study the self-assembly<sup>9</sup> and packing<sup>10</sup> of anisotropic colloids.

When derived directly from molecular species, nonspherical microparticles at the colloidal length scale such as cubes, rods, and disks are obtained by controlling the growth and nucleation steps during precipitation<sup>11</sup> or by making second-generation colloids using high-quality templates.<sup>12</sup> The first method does not produce monodisperse colloids<sup>2</sup> and is hampered by the fact that there is no control over the specific shapes obtained, which are highly dependent on minute changes in experimental conditions.<sup>11</sup> Creating material from templates is a batch process that is dependent on the use of high-quality templates that might not be readily available for all nonspherical shapes of interest. Nonspherical microparticles can also be formed indirectly from their spherical precursors by deforming monodisperse polymeric spheres using external forces,<sup>12</sup> which, besides being a batch process, also necessitates the creation of spherical microparticles before nonspherical ones can be created.

In this work, we demonstrate that microfluidics offers a convenient and finely controllable route to synthesizing nonspherical microparticles with the twin advantages of using soft lithography to design desired geometries and of the ability to exploit fluid mechanics to tune particle morphology. The complex patterns obtained as a result of the instability and nonlinearity in two-phase flow<sup>5</sup> are an example of how fluid mechanics can be exploited to create novel shapes that are very difficult to create using the methods described so far. When using microfluidic synthesis, particle size can be tuned continuously by modifying the flow parameters in the microfluidic channel. Furthermore, the particle surface properties can be modified after formation by using the layer-by-layer technique.<sup>13</sup>

Recently, microfluidics has been used as a means to create polymeric microspheres with a narrow size distribution.<sup>14,15,16</sup> Droplets of a dispersed phase that is either

\* Author to whom correspondence should be addressed. Tel: 617-253-4534. Fax: 617-258-5042. E-mail: pdoyle@mit.edu.

(1) Russel, W. B.; Saville, D. A.; Schowalter, W. R. *Colloidal Dispersions*, 1st ed.; Cambridge University Press: New York, 1989; Chapter 1.

(2) Yin, Y.; Xia, Y. *Adv. Mater.* **2001**, *13*, 267–271.

(3) Xia, Y.; Gates, B.; Yin, Y.; Lu, Y. *Adv. Mater.* **2000**, *12*, 693–713.

(4) Anna, S. L.; Bontoux, N.; Stone, H. A. *Appl. Phys. Lett.* **2000**, *82*, 364–366.

(5) Thorsen, T.; Roberts, R. W.; Arnold, F. H.; Quake, S. R. *Phys. Rev. Lett.* **2001**, *86*, 4163–4166.

(6) Nisisako, T.; Torii, T.; Higuchi, T. *Lab Chip* **2002**, *2*, 24–26.

(7) Jogun, S. M.; Zukoski, C. F. *J. Rheol.* **1999**, *43*, 847–871.

(8) Brooks, C. F.; Fuller, G. G.; Frank, C. W.; Robertson, C. R. *Langmuir* **1999**, *15*, 2450–2459.

(9) Adams, M.; Dogic, Z.; Keller, S. L.; Fraden, S. *Nature* **1998**, *393*, 349–352.

(10) Donev, A.; Stillinger, F. H.; Chaikin, P. M.; Torquato, S. *Phys. Rev. Lett.* **2004**, *92*, 255506.

(11) Matijevic, E. *Langmuir* **1994**, *10*, 8–16.

(12) Jiang, P.; Bertone, J. F.; Colvin, V. L. *Science* **2001**, *291*, 453–457.

(13) Caruso, F.; Lichtenfeld, H.; Giersig, M.; Mohwald, H. *J. Am. Chem. Soc.* **1998**, *120*, 8523–8524.

(14) Sugiura, S.; Nakajima, M.; Tong, J.; Nabetani, H.; Seki, M. *J. Colloid. Interface Sci.* **2000**, *227*, 95–103.

(15) Sugiura, S.; Nakajima, M.; Seki, M. *Ind. Eng. Chem. Res.* **2002**, *41*, 4043–4047.

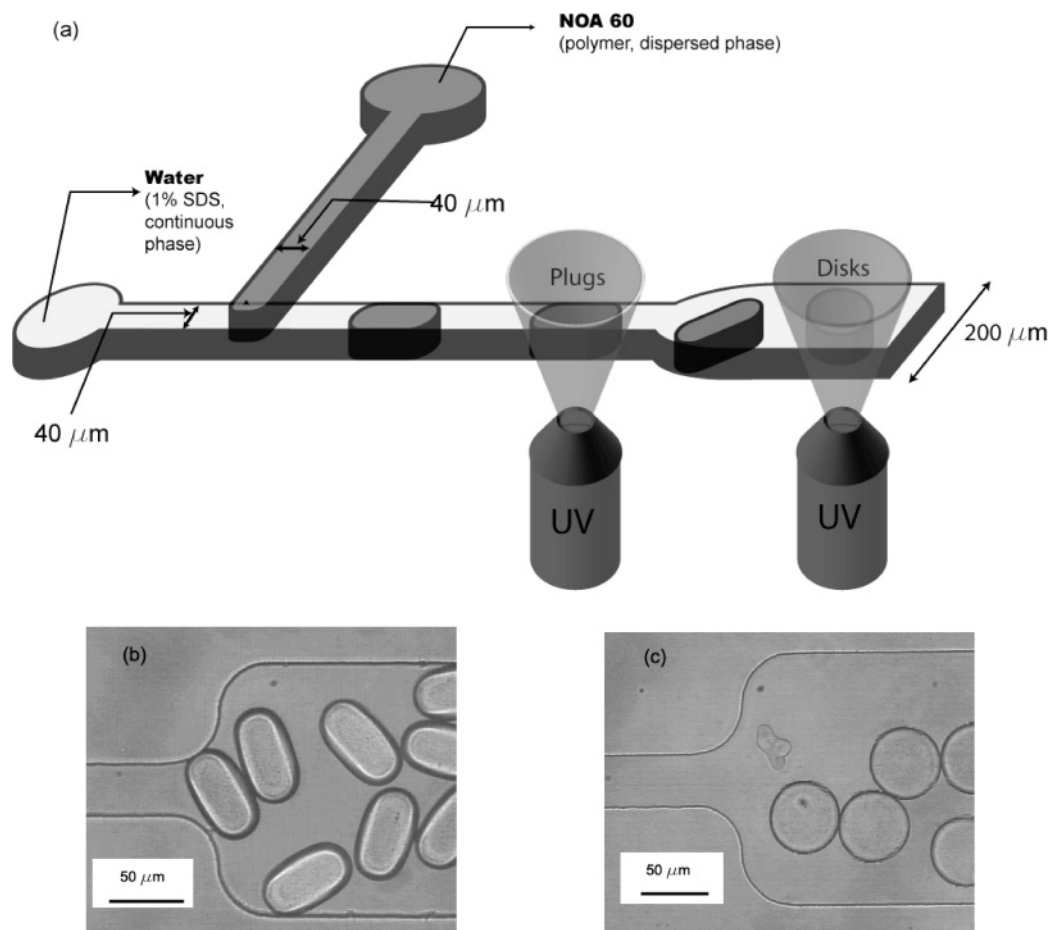


**Figure 1.** Microchannel geometry used to create plugs and disks: (a) schematic of channel with plug and disk creation zones marked; (b) polymerized plugs in the 200  $\mu\text{m}$  section of the channel, 38  $\mu\text{m}$  height; and (c) polymerized disks in the 200  $\mu\text{m}$  section of the channel, 16  $\mu\text{m}$  height.

a low-melting-point lipid<sup>14</sup> or a UV-curable polymer<sup>15,16</sup> are pinched off into a continuous aqueous phase and are then either frozen or polymerized to create solid spheres. Precisely sized solid spheres can be obtained by tuning the flow of the dispersed and continuous phases to form colloids of a desired size. In addition to forming microspheres, UV-curable polymers have also been used to freeze flow instabilities with macroscopic feature sizes.<sup>17</sup>

In this work, droplets of a UV-curable polymer were first formed at a T-junction by shearing the dispersed polymer phase using a continuous, surfactant-containing aqueous phase (Figure 1a). The droplets formed were confined into plug- and disklike shapes by utilizing suitable microchannel geometries before the polymer was cured in situ using UV light from the objective of the microscope to preserve the nonspherical shapes. Both plugs and disks were created using the basic microchannel geometry illustrated in Figure 1a, the only difference between the two channels used being their height, which was 38  $\mu\text{m}$  to form plugs and 16  $\mu\text{m}$  to form disks. Plugs were formed by polymerizing slugs during their confined passage through the 40  $\mu\text{m}$  section of the channel, while disks were formed by polymerizing slugs that had relaxed into a disklike shape, due to the minimization of interfacial energy, in the 200  $\mu\text{m}$  section of the channel (Figure 1a). As in the case with polymeric microspheres, the sizes of the plugs and disks formed were tuned by controlling the flow rates of the dispersed and continuous phases. The

formation of plugs and disks is demonstrated here as a proof-of-principle to show that nonspherical microparticles can be successfully synthesized in microchannels.

### Experimental Methods

Microfluidic channels were fabricated by pouring polydimethylsilyl silane (PDMS, Sylgard 184, Dow Corning) on a silicon wafer containing positive-relief channels patterned in SU-8 photoresist (Microchem). The channel dimensions are shown in Figure 1a. Channels of two different heights were used—38  $\mu\text{m}$  to create plugs and 16  $\mu\text{m}$  to create disks. The microdevices were sealed to glass slides using a PDC-32G plasma sterilizer (Harrick).

Syringe pumps (KDS 100, KD Scientific) were used to adjust the flow rates of the two phases. Both aqueous and polymer solutions were infused into the channels using 50 or 100  $\mu\text{L}$  Hamilton Gastight syringes (1700 series, TLL). The continuous phase was a 1% SDS solution that had been prefiltered using a 0.2  $\mu\text{m}$  filter. The viscosity of the SDS solution ( $\mu = 1.08$  mPa s) was measured using a glass capillary viscometer (Technical Glass Products). Norland Optical Adhesive 60 (NOA 60, Norland Products,  $\mu = 300$  mPa s), a UV-sensitive liquid photopolymer that cures when exposed to UV light, was used as the dispersed phase. An energy flux of 3  $\text{J}/\text{cm}^2$  was required for a full cure.

The formation of the microparticles was visualized using a CCD camera (KPM1A, Hitachi) mounted on an inverted microscope (Axiovert 200, Zeiss). Images were captured and processed using NIH Image software. Plug length calculations were performed in NIH Image by measuring the longest observable dimension of the plug. A 100 W HBO mercury lamp served as the energy source. A UV filter set that provides wide UV excitation (11000v2: UV, Chroma) was used to generate light of the desired wavelength. The interfacial tension between the SDS solution and the polymer was measured to be 6.64 mN/m by the pendant drop method using a DSA10 Tensiometer (Kruss).

(16) Nisisako, T.; Torii, T.; Higuchi, T. *Chem. Eng. J.* **2004**, *101*, 23–29.

(17) Li, M.; Xu, S.; Kumacheva, E. *Langmuir* **2000**, *16*, 7275–7278.

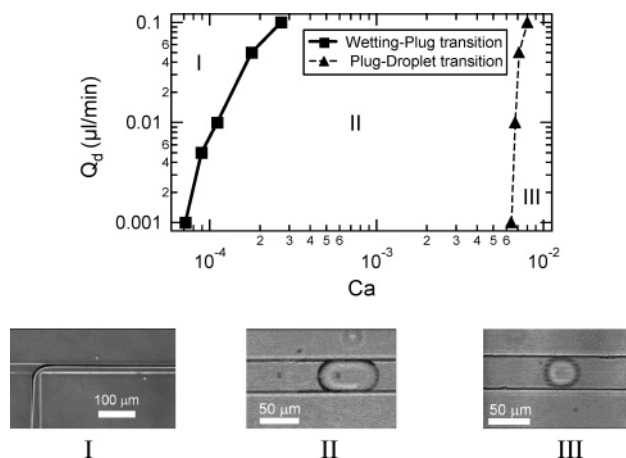


**Figure 2.** Phase plot of the system with the three labeled phases shown: (I) wetting phase, (II) plug phase, and (III) droplet phase. The wetting–plug transition, which is abrupt, is shown as a solid line. The plug–drop transition, which is more gradual, is shown as a dashed line. The symbols shown on these lines were experimentally obtained by fixing  $Q_d$  and gradually increasing  $Ca$  until a change of phase was observed. The lines that connect these symbols are drawn to guide the eye. The uncertainty in the location of the transition is comparable to the size of the symbol. Furthermore, the transitions are independent of the experimental path taken (i.e., increasing or decreasing  $Ca$ ).

### Results and Discussion

The break-off of droplets at a T-junction is governed by the competition between viscous stress and surface tension. The Capillary number  $Ca = \mu v_c / \gamma$ , is a measure of the relative importance of these two effects, where  $\mu$  is the viscosity of the continuous phase,  $v_c$  is the superficial velocity of the continuous phase, and  $\gamma$  is the interfacial tension between the continuous and the dispersed phases. The droplet size obtained at the T-junction can be tuned by modifying  $Ca$ .<sup>5</sup>

In our system,  $Ca$  can be modified by changing  $Q_c$  the flow rate of the continuous phase, which leads to a change in  $v_c$  through  $v_c = Q_c/A$ , where  $A$  is the area of cross-section of the microchannel. As  $Ca$  increases, the shear forces increase in comparison to the surface tension forces, leading to the formation of smaller droplets. In addition to  $Ca$ , the flow rate of the dispersed phase  $Q_d$  (and hence the velocity of the dispersed phase,  $v_d = Q_d/A$ ), can also be used to tune droplet size for droplet break-off at a T-junction. As  $Q_d$  increases at a constant value of  $Ca$ , droplets of larger size are formed. Previous work on droplet breakoff in microfluidics has used a phase diagram to represent the different regimes observed, as a function of experimental parameters.<sup>4,5,18,19</sup> Using a similar approach, we plotted the phase behavior of our system in  $Ca$ – $Q_d$  coordinates. As shown in Figure 2, we have classified the system into three phases—the wetting phase (I), the plug phase (II), and the droplet (III) phase. The wetting phase is characterized by the polymer flowing as one phase through the channel and occurs at very low  $Ca$  when the shear forces are not sufficiently large to cause the polymer phase to pinch off at the T-junction. As  $Ca$  is gradually increased at a constant  $Q_d$ , a critical capillary number ( $Ca_{w-p}$ ) is reached where plugs of polymer begin to pinch-off at the T-junction. This represents the transition from the *wetting* phase to the *plug* phase. For  $Ca > Ca_{w-p}$ , the

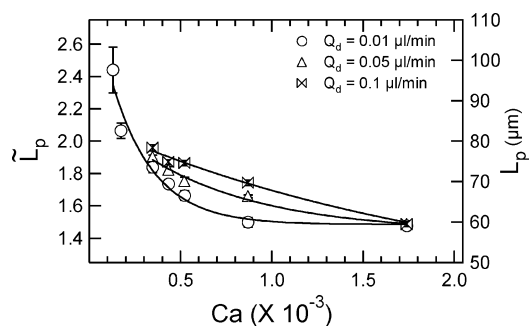


**Figure 3.** Plug length plotted as a function of  $Ca$  for different values of  $Q_d$ . On the left axis is plotted the dimensionless plug length,  $\tilde{L}_p (L_p/40 \mu\text{m})$ . On the right axis is plotted, the measured plug length,  $L_p (\mu\text{m})$ .

dispersed phase starts breaking off at the T-junction, and at these still relatively low values of  $Ca$ , the diameter of the resulting droplets is larger than the width of the channels leading to plugs rather than droplets being cleaved off. As  $Ca$  is further increased, plugs of progressively decreasing length are formed, leading eventually to the formation of droplets ( $L < 38 \mu\text{m}$ ). The droplet phase is thus an extension of the plug phase but is classified separately because we are interested in the formation of nonspherical shapes. This transition to the droplet phase ( $Ca_{p-d}$ ) occurs at values of  $Ca$  that are one or two orders of magnitude larger than the  $Ca_{w-p}$  at the same  $Q_d$ . As is intuitively expected, both  $Ca_{w-p}$  and  $Ca_{p-d}$  increase with increasing  $Q_d$ . The phase plot shown in Figure 2 is a useful engineering tool to define the operating regimes of the microfluidic device.

Plug length,  $L_p$ , was controlled by changing  $Ca$  and  $Q_d$ . Plug lengths are nondimensionalized using the width of the channel and are given by  $\tilde{L}_p = L_p/40 \mu\text{m}$ . As  $Ca$  is increased within the plug phase at a given  $Q_d$ , plugs of decreasing length,  $L_p$ , are observed (Figure 3) until the length of the plugs equals the width of the channel, signaling the onset of the droplet phase. The plug length drops very gradually at  $Ca > 0.001$ , and thus only the range of  $Ca$  where a significant drop in plug length is seen has been shown in Figure 3. Plug length can also be modified by changing  $Q_d$ . For a given value of  $Ca$ , a higher  $Q_d$  leads to a larger plug length. In all cases, the plug lengths obtained had a standard deviation of less than 5%.

For a given  $Q_d$ , the plugs of the greatest length were observed at low values of  $Ca$  just when the transition from wetting to the plug phase occurs. Due to the nonsteady motion of the syringe pump at low flow rates, the region where extremely long plugs are obtained could not be probed in depth.

After the plugs were formed, they had to be polymerized before they reached the  $200 \mu\text{m}$  section where they would otherwise relax into a disk like shape. Plugs were polymerized just before they entered the  $200 \mu\text{m}$  section (Figure 1a) so that there was the least chance of their blocking the channels. A small layer of lubricating water film around the plug rendered the plug mobile even after it was polymerized.<sup>20</sup> Two of the three dimensions of the plug are dictated by channel geometry—namely the height ( $38 \mu\text{m}$ ) and the width ( $40 \mu\text{m}$ ) of the channel. Thus, two of the dimensions of the plug were fixed at  $38 \mu\text{m}$  and  $40 \mu\text{m}$ , while the plug length was a function of  $Ca$  and  $Q_d$ . By choosing an appropriate combination of  $Ca$  and  $Q_d$ , plugs of a desired length were obtained. The plug seen in Figure 4a was obtained at  $Q_d = 0.05 \mu\text{L}/\text{min}$  and  $Ca = 1.6$

(18) Tice, J. D.; Lyon, A. D.; Ismagilov, R. *Anal. Chim. Acta.* **2004**, *507*, 73–77.

(19) de Mas, N.; Gunther, A.; Schmidt, M. A.; Jensen, K. F. *Ind. Eng. Chem. Res.* **2003**, *42*, 698–710.

(20) Bico, J.; Quere, J. J. *Fluid Mech.* **2002**, *467*, 101–127.



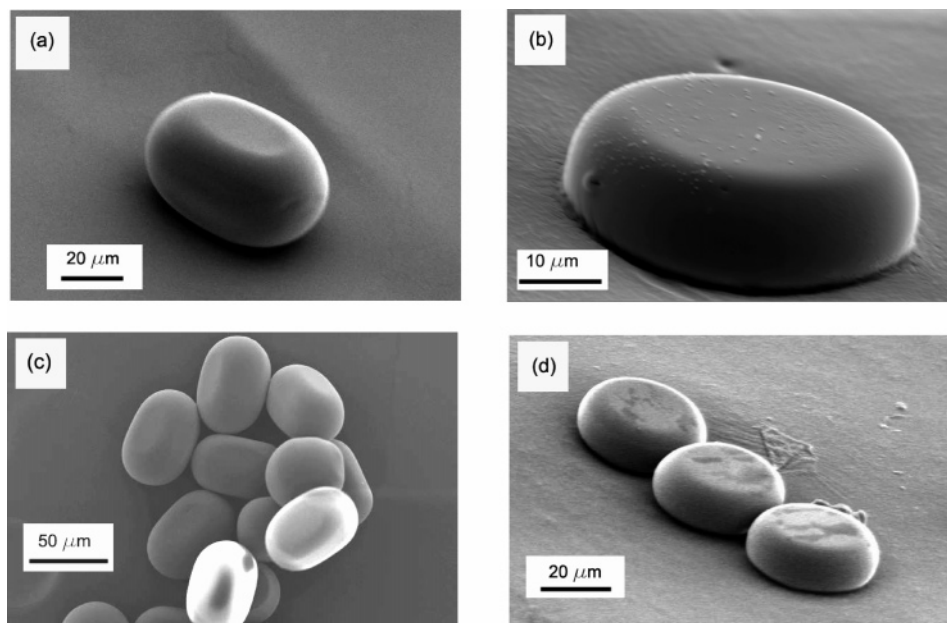


**Figure 4.** SEM images of nonspherical colloids: (a) plug formed at  $Q_d = 0.05 \mu\text{L}/\text{min}$  and  $Ca = 1.6 \times 10^{-3}$ ; (b) disk formed at  $Q_d = 0.05 \mu\text{L}/\text{min}$  and  $Ca = 4.8 \times 10^{-3}$ ; (c) collection of plugs formed at  $Q_d = 0.05 \mu\text{L}/\text{min}$  and  $Ca = 1.6 \times 10^{-3}$ ; and (d) collection of disks formed at  $Q_d = 0.05 \mu\text{L}/\text{min}$  and  $Ca = 9.6 \times 10^{-3}$ .

$\times 10^{-3}$ . A collection of plugs is shown in Figure 4c. The cured polymer is stable indefinitely,<sup>21</sup> and we expect no change in the structure of the plugs obtained after they are formed.

The low surface area of the plugs ( $\sim 10^{-5} \text{ cm}^2$ ) and the high energy flux provided by a 100 W UV lamp meant that even a very small exposure time ( $< 1 \mu\text{s}$ ) was sufficient to polymerize the plugs, given that an energy input of only  $3 \text{ J}/\text{cm}^2$  is required for a full cure. On the other hand, very long exposure times led to plugs sticking to the PDMS or the glass slide resulting in blockages. The area of focus of the UV lamp and its intensity were progressively reduced from their maximum possible values until polymerized plugs could be obtained steadily in the channel. It was verified that the polymerization of the plugs did not lead to any modification in the dynamics of the system by measuring plug lengths before and after polymerization was initiated. This is most likely due to the fact that the flow rates of the streams are imposed by the syringe pump, which compensates for pressure variations within the system that may be caused upon curing of the polymer.

Other authors have reported the formation of pear-shaped,<sup>22</sup> pearl-necklace-shaped,<sup>5,22</sup> and ribbon-shaped<sup>5</sup> objects that could also then be polymerized to synthesize different nonspherical shapes. To show that this method can be extended to create other shapes, we obtained disks by using a channel identical to that used to create plugs, changing only the height of the channel to  $16 \mu\text{m}$ . As shown in Figure 1c, disks were obtained by polymerizing plugs that had relaxed into a disklike configuration in the  $200 \mu\text{m}$  section of the channel. One of these disks is shown in Figure 4b, while a collection of them is shown in Figure 4d. It is noteworthy that there is no visible curvature on the disk surface, leading to microparticles that have a flat surface. The height of the disk seen in Figure 4b is  $16 \mu\text{m}$ , while the diameter is  $40 \mu\text{m}$ .

## Conclusion

A new microfluidics-based approach has been demonstrated that offers a convenient route to generate nonspherical microparticles. This process has the potential to continuously synthesize monodisperse nonspherical colloids in a variety of shapes using a combination of soft lithography and complex pattern formation seen in two-phase flows. As a proof of principle, monodisperse polymeric plugs and disks of different sizes were fabricated. The operational phase space of the microfluidic device was also characterized. Using this method, the material properties of the colloids can be altered by using different photopolymers (e.g., photopolymerizable PEG gels), while size and/or morphology can be adjusted by tuning fluid flow properties or the microchannel geometry. The creation of faceted shapes could allow for surface features that may be useful for fundamental studies on particle–surface interactions and also allow for the creation of designer colloids for special applications. The microparticles synthesized in this study were larger than  $10 \mu\text{m}$ , but particles in the colloidal size range ( $< 10 \mu\text{m}$ ) may be formed by further scaling down the device. For example, using existing soft lithography methods, it is feasible to scale down the current device to have channel widths of  $10 \mu\text{m}$  and a height of a few micrometers. Further investigations on combining different materials and microchannel geometries are also underway to utilize this method to create nonspherical colloids with novel morphologies and properties. Additional work on scaling up the process will also be needed to generate large volumes of nonspherical colloids that will be needed to characterize their phase behavior and rheological properties.

**Acknowledgment.** We gratefully acknowledge the support of NSF NIRT Grant No. CTS-0304128 for this project.

(21) Norland Products Technical Literature; <https://www.norlandprod.com/techrpts/agetest.html>.

(22) Dreyfus, R.; Tabeling, P.; Willaime, H. *Phys. Rev. Lett.* **2003**, *90*, 144505.